© 2022. Published by The Company of Biologists Ltd | Journal of Experimental Biology (2022) 225, jeb243828. doi:10.1242/jeb.243828

RESEARCH ARTICLE

The trunk–tail junctional region in *Ciona* larvae autonomously expresses tail-beating bursts at ∼20 second intervals

Takashi Hara[1,*], Shuya Hasegawa[1,*], Yasushi Iwatani[2] and Atsuo S. Nishino[1,3,‡]

ABSTRACT

Swimming locomotion in aquatic vertebrates, such as fish and tadpoles, is expressed through neuron networks in the spinal cord. These networks are arranged in parallel, ubiquitously distributed and mutually coupled along the spinal cord to express undulation patterns accommodated to various inputs into the networks. While these systems have been widely studied in vertebrate swimmers, their evolutionary origin along the chordate phylogeny remains unclear. Ascidians, representing a sister group of vertebrates, give rise to tadpole larvae that swim freely in seawater. In the present study, we examined the locomotor ability of the anterior and posterior body fragments of larvae of the ascidian *Ciona* that had been cut at an arbitrary position. Examination of more than 200 fragments revealed a necessary and sufficient body region that spanned only ∼10% of the body length and included the trunk–tail junction. 'Mid-piece' body fragments, which included the trunk–tail junctional region, but excluded most of the anterior trunk and posterior tail, autonomously expressed periodic tail-beating bursts at ∼20 s intervals. We compared the durations and intervals of tail-beating bursts expressed by mid-piece fragments, and also by whole larvae under different sensory conditions. The results suggest that body parts outside the mid-piece effect shortening of swimming intervals, particularly in the dark, and vary the burst duration. We propose that *Ciona* larvae express swimming behaviors by modifying autonomous and periodic locomotor drives that operate locally in the trunk–tail junctional region.

KEY WORDS: Locomotion, Tadpole larva, Ascidian, Tunicate, Swimming, Pacemaker

INTRODUCTION

Regulatory mechanisms for locomotion, such as swimming, walking or flying, have been extensively examined in vertebrate animals. The findings obtained showed that the functional elements forming locomotion patterns are sufficiently equipped in the spinal cord. The operational mechanisms of the spinal cord to express swimming locomotion patterns have been investigated using lamprey, teleosts and amphibian larvae (for reviews, see Grillner et al., 1991; Roberts et al., 2010; Fetcho and McLean, 2010). Isolated pieces of fish and tadpole spinal cords express coordinated 'fictive' swimming patterns (e.g. Cohen and Wallén, 1980; Cangiano and Grillner, 2003, 2005). Therefore, neural circuits in the spinal cord fulfill the definition of a central pattern generator (CPG) as elements in the central nervous system (CNS) that generate a rhythmic and stereotypic output for locomotion in the absence of afferent input or feedback (e.g. Delcomyn, 1980, 1998). Previous studies revealed that the basic circuits expressing fictive swimming are not localized; instead, they are arranged in parallel, ubiquitously distributed, and mutually coupled in the spinal cord for the propagation of reciprocal activities down the long axis (e.g. Buchanan and Grillner, 1987; Cangiano and Grillner, 2003, 2005 Wiggin et al., 2012, 2014).

It is also known that these circuits in the spinal cord do not operate in an autonomous manner, but are driven in response to descending inputs from superior brain centers (e.g. the reticular formation and midbrain locomotor region) or afferent inputs from cutaneous sensory systems (for reviews, see Tytell et al., 2011; Grillner and El Manira, 2020) or by the application of excitatory amino acids and their analogs, such as D- or L-glutamate, D-aspartate, and *N*-methyl-D-aspartate (Cohen and Wallén, 1980; Poon, 1980; Grillner and Wallén, 1984; Dale and Roberts, 1984). Previous studies demonstrated that evoked fictive swimming bursts emerged periodically and were separated by intervals, even when the spinal cord was tonically stimulated by chemical activators (Cangiano and Grillner, 2003; Wiggin et al., 2012).

While the fundamental mechanisms that form swimming locomotion are shared from lamprey to teleosts and amphibian tadpoles (Fetcho and McLean, 2010; Roberts et al., 2010; Grillner and El Manira, 2020), their origin along the chordate phylogeny has not yet been elucidated. Ascidians [Class Ascidiacea, Subphylum Tunicata (previously known as Subphylum Urochordata)] are marine invertebrate animals included in the sister clade of vertebrates that constitute a group in the phylum Chordata (or the superphylum Chordata; Satoh et al., 2014). Adult ascidians are sessile and benthic, but give rise to tadpole-shaped larvae. Ascidian larvae share basic bodyplans with those of vertebrates, including the axial notochord, dorsal neural tube and bilateral muscle bands in the tail (Kowalevsky, 1866; Katz, 1983; Satoh, 2003; Meinertzhagen et al., 2004), and exhibit a sophisticated swimming performance (Crisp and Ghobashy, 1971; Svane and Young, 1989; McHenry and Patek, 2004; Nishino et al., 2011; Salas et al., 2018).

The simplified architecture of larvae, composed only of thousands of cells, represents a miniature form of the chordate bodyplan (e.g. Satoh, 2003; Meinertzhagen et al., 2004). In the larva of *Ciona*, an experimental model of ascidians, 18 electrically coupled muscle cells are situated on each of the left and right sides in the tail. The three-row arrangement (i.e. dorsal, medial and ventral rows) of the muscle cells is bilaterally mirror imaged and invariant among individuals (Bone, 1992; Passamanech et al., 2007; Nishino et al., 2011; Razy-Krajka and Stolfi, 2019). Approximately 180 neurons have been identified in the larval CNS, and the number, position and connections of their

[1]Department of Biology, Graduate School of Agriculture and Life Science, Hirosaki University, Hirosaki 036-8561, Japan. [2]Department of Science and Technology, Graduate School of Science and Technology, Hirosaki University, Hirosaki 036-8561, Japan. [3]Department of Bioresources Science, United Graduate School of Agricultural Sciences, Iwate University, Hirosaki 036-8561, Japan.
*These authors contributed equally to this work

‡Author for correspondence (anishino@hirosaki-u.ac.jp)

Y.I., 0000-0003-1446-8176; A.S.N., 0000-0003-2818-4377

Received 23 November 2021; Accepted 3 June 2022

subtypes are presumed to be mostly constant among individuals (Ryan et al., 2016; Hudson, 2016; Nishino, 2018).

Connectome analyses performed by Ryan et al. (2016) revealed 143 neurons within an anterior ganglion in the trunk, called the brain vesicle (BV), which contains a gravity sensor (called the otolith), photoreceptor (ocellus) and associated pigment cells. Twenty-five neurons were found in another ganglion, called the motor ganglion (MG), positioned at the trunk–tail junction (Ryan et al., 2016, 2017). The MG has been assumed to constitute an essential component that directs the beating of the tail. This is because this ganglion contains the cell bodies of motoneurons, which extend their axon posteriorly along the caudal nerve cord (CNC) and innervate tail muscle cells (Okada et al., 2002; Nishino et al., 2010; 2011; Stolfi and Levine, 2011; Ryan et al., 2016, 2017).

Posterior to the MG, the CNC runs along the dorsal side of the notochord in the tail. Approximately nine neurons are distributed on the CNC. Because of the scarcity of neurons, this region has not been expected to play an essential role in the formation of locomotion patterns (Katz, 1983; Bone, 1992; Ryan et al., 2016; 2017). Two recently identified pairs of neurons located close to the MG, called the ascending contralateral inhibitory neurons (ACINs), are an exception (Horie et al., 2010). The ACINs, which are presumed to be glycinergic, have been shown to extend commissural axons to contralateral motor axons for inhibiting activity on the contralateral side (Horie et al., 2010; Nishino et al., 2010; Nishitsuji et al., 2012). Their characteristics are similar to those of some types of commissural inhibitory neurons in the vertebrate spinal cord (Liao and Fetcho, 2008; Roberts et al., 2010; Satou et al., 2020). Several pairs of mid-tail neurons (MTNs) are another or potentially the only other central neuron type in the CNC (Imai and Meinertzhagen, 2007; Ryan et al., 2016). MTNs are presumed to be cholinergic and may innervate tail muscle cells (Imai and Meinertzhagen, 2007; Horie et al., 2010; Nishino et al., 2011).

Despite the accumulation of structural information, the functional aspects of the *Ciona* larval CNS remain unclear. It has not yet been established whether neurons in the MG and the ACINs comprise a necessary and sufficient element for the expression of swimming locomotion. A CPG is strictly defined as neural circuits in the CNS that generate output signals for a stereotypical motor pattern under conditions where proprioceptive or sensory feedback is completely excluded (e.g. Delcomyn, 1980, 1998). As *Ciona* larvae are as small as ∼1 mm, difficulties are associated with the exclusion of potential sensory paths and exclusively recording output signals from the CNS.

Although it has not yet been confirmed whether a pure CPG is present in the *Ciona* larval CNS, the part of the body expressing rhythmic tail beating can still be examined. Therefore, we herein performed a series of experiments in which the larval body was fragmented at an arbitrary position, and movement patterns expressed by the anterior and posterior pieces of the body were then examined. The results obtained demonstrate the necessary and sufficient role of the trunk–tail junctional region harboring the MG and ACINs. 'Mid-piece' body fragments, which included the trunk–tail junction, but excluded the trunk region anterior to the MG as well as the posterior half or more of the tail, expressed reciprocal tail-beating bursts in an autonomous manner, i.e. without any exogenous stimulators. We also found that these mid-piece fragments expressed tail-beating bursts highly periodically at ∼20 s intervals. We compared these temporal patterns expressed by mid-piece fragments with those expressed by whole bodies with their displacement limited using methylcellulose seawater. Based on the results obtained, we concluded that the *Ciona* larva has an autonomously and periodically operating functional unit that drives tail-beating bursts in the trunk–tail junctional region, and swimming behaviors expressed by the whole *Ciona* larva are represented by modifications of the autonomous activity in this local unit through descending and afferent inputs from outside the region.

MATERIALS AND METHODS

Animals

Mature adults of *Ciona intestinalis* (Linnaeus 1767) (called type A), which Brunetti et al. (2015) recently defined as *Ciona robusta* Hoshino and Tokioka 1967, were obtained from populations reared in the Misaki Marine Biological Station, The University of Tokyo (Miura, Japan) or the Maizuru Fisheries Research Station, Kyoto University (Maizuru, Japan) via the National BioResource Project, AMED, Japan. They were kept in 5 l laboratory tanks containing artificial seawater (ASW; Marine Art BR, Osaka-Yakken, Japan) or a mixture of ASW with natural seawater. Seawater in the tanks was gently stirred using a paddle connected to a synchronous motor (15 rpm, Nidec Servo, Kiryu, Japan). Tanks were placed in an air-conditioned room (18–19°C) and kept under constant light to prevent the uncontrolled release of gametes. Ascidians are hermaphroditic, and mature eggs and sperm obtained from different adults were cross-fertilized as previously described (Jokura et al., 2020). Fertilized eggs were reared in a cool incubator set at 18°C. Tadpole-shaped larvae hatched out at approximately 17–18 h post-fertilization (hpf).

Preparation of anterior and posterior fragments of *Ciona* larvae

Hatched larvae with a normal well-elongated tail (≤24 hpf) were selected and placed in ASW in a Petri dish coated with silicone rubber (SYLGARD 184, Dow Corning). If required, an image of a larva to be cut was taken in advance with a digital camera (DiFi2, Nikon) or video camera (HDR-CX420, Sony) mounted on a stereomicroscope (SMZ745T, Nikon) or with a digital high-speed camera (VCC-1000, Digimo, Tokyo, Japan) mounted on another stereomicroscope (MZ FLIII, Leica). When the larva ceased swimming, the larval body was cut into anterior and posterior fragments using Vannas micro scissors (Type 501790, World Precision Instruments) at an arbitrary position. After cutting, images of the anterior and posterior fragments were taken again using the same photosystem, and the lengths of the total body, anterior fragment and posterior fragment were subsequently measured on a PC to identify the approximate position of the cut site using the Bohboh image analyzer (v.3, Bohboh Software) or ImageJ (v.1.52a or v.1.53c). Cut sites are represented herein as the relative location (%) on a scale set along the longitudinal axis of the body, in which the position of the trunk–tail junction was defined as 0% and that of the tail tip (excluding the larval tunic) as 100%. Cut sites in the trunk were represented by negative values (see Results). The values for cut sites were calculated by dividing the length of the remaining tail (when the cut site was in the tail) or the remaining trunk (when the cut site was in the trunk) by the tail length before cutting. In the course of data analysis, we noted that the sum of the lengths of the anterior and posterior fragments after cutting was shorter than the sum of the lengths of the trunk and tail before cutting (94.9±3.1%, mean±s.d., n=125; samples represented in Fig. 1). Therefore, our estimation of cut sites showed slightly lower values by approximately 5% (e.g. ∼95% for 100% or ∼9.5% for 10%). In addition, other potential deformations of the fragments and/or variation in internal structures among specimens (e.g. variation in the anteroposterior location of particular neuron types) were considered. Because both of these potential errors were difficult to evaluate, we herein present the raw values for cut sites derived from the relative lengths of the remaining tail or trunk in the fragments.

Journal of Experimental Biology (2022) 225, jeb243828. doi:10.1242/jeb.243828

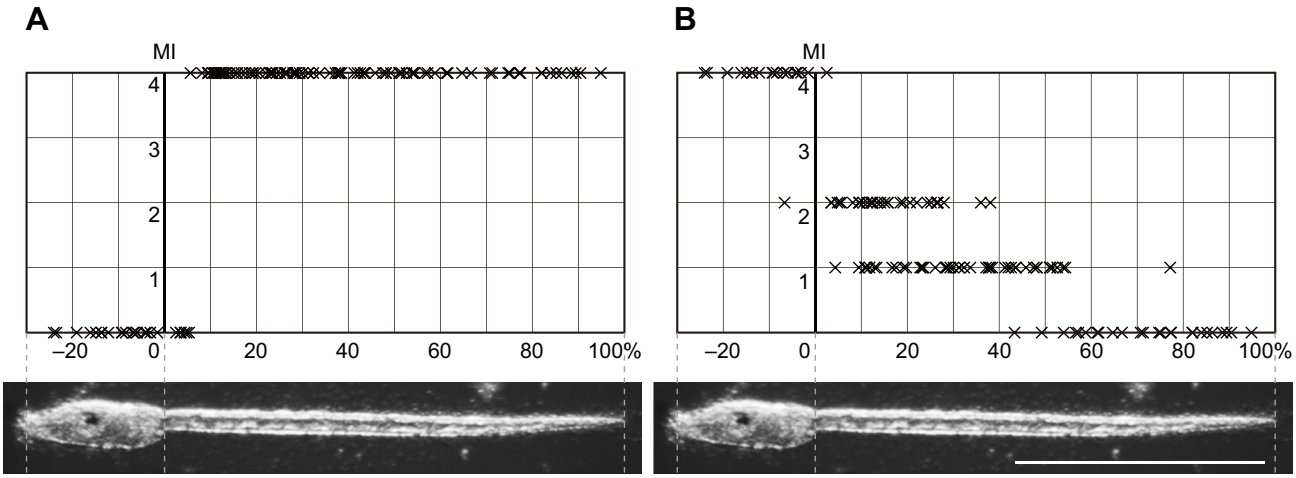

Fig. 1. Locomotion ability of anterior and posterior fragments of segmented *Ciona* larvae. (A,B) Evaluated ability of movement by the anterior (A; *n*=125 fragments examined) and posterior (B; *n*=125) fragments. The vertical axis indicates in motion index (MI) values (see Table 1). Cut sites (marked by crosses) are indicated along the horizontal axis, which is defined as 0% at the trunk–tail junction and 100% at the tail tip. Images of a *Ciona* larva are shown at the bottom for reference. Scale bar: 500 µm.

The anterior and posterior fragments were both placed in another Petri dish covered with silicone rubber containing ASW or ASW with 100 µmol l^{-1} L-glutamate (L-Glu; prepared from glutamic acid monosodium salt, Fujifilm Wako). After acclimation to the solution for at least 20 min, movement patterns expressed by the anterior and posterior fragments were captured by the video camera or high-speed camera mounted on the stereomicroscope (as described above), and movement patterns were evaluated by direct observation or observation of movies. We categorized movement patterns into five levels, 0–4, called herein 'motion index' (MI) values (Table 1). When tail beats in a swimming burst were bilaterally alternating and regularly rhythmic, we evaluated the motion ability of the fragment as MI=4. When tail beats were rhythmic but unilateral, the ability was categorized as MI=3. If burst-like serial contractions (≥3 times s^{-1}) were observed, but their timing was irregular, the movement ability of the fragment was defined as MI=2. When only sporadic contractions (<3 times s^{-1}) occurred, the fragment was categorized as MI=1. When there was no movement for 5 min, we defined the MI of the fragment as 0 (Table 1). The MI values of the anterior and posterior fragments were plotted against the cut sites. In the present study, we considered fragments categorized as MI=4 to possess sufficient components for swimming locomotion. Conversely, we considered that fragments categorized as MI=0–3 lacked some necessary (or required) elements and were insufficient to express a locomotion pattern.

Preparation of mid-piece fragments

Mid-piece fragments were defined as the body part from which the anterior trunk including the BV and the posterior half (or more) of the tail were both excluded, but which retained MI=4. To prepare these fragments, the posterior half of the tail of hatched larvae (≤24 hpf) was initially removed and the anterior portion of the trunk was then amputated in order to exclude the BV using the same tools as those described above. The location of the BV was identified by pigmentation in the otolith and ocellus (Katz, 1983), and we intended to sufficiently exclude the posterior BV region, which is important for controlling motor behaviors (Kourakis et al., 2019). After we confirmed that MI=4, mid-piece fragments were placed in ASW or ASW containing 1% methylcellulose 4000 (1% MC, Fujifilm Wako), 100 µmol l^{-1} L-Glu or 1 mmol l^{-1} L-Glu. The movements of mid-piece fragments were recorded for 20 min by the video camera mounted on the stereomicroscope. By observing recorded movies, the number of events was counted and the cumulative duration of tail-beating bursts was measured.

Mid-piece fragments were prepared from hatched larvae at 19–20 or 22–24 hpf by the procedure described above and their movement patterns were analyzed in detail. Movements expressed by mid-piece fragments were recorded as described above for 20 min and were later analyzed on a PC. Movie files recorded by the video camera (HDR-CX420, Sony or GZ-F270-W, JVC) were exported as sequential images at 30 frames s^{-1} using a locally developed application running on a Windows PC. Images were imported into ImageJ (v.1.53c), and changes in 8-bit grayscale brightness (0–255) at a 'point of interest' (POI) were visualized. When the larval tail beats on an image sequence, the shade of the tail traverses the POI as many times as the tail beats, and, thus, brightness at the POI changes according to the movement of the tail. We also used the high-speed video camera (VCC-1000, Digimo) to calculate the tail-beating frequency at a higher resolution of time (250 frames s^{-1}). To evaluate the durations and intervals of tail-beating bursts, sporadic contractions, including flick-like movements, were excluded, and swimming-like bursts of regular bilateral tail beating (well-patterned movements) were considered.

Table 1. Motion index (MI) to evaluate movements expressed by larval fragments

MI	Characteristics of movements
4	Swimming-like bursts that are bilaterally and regularly rhythmic
3	Rhythmic tail beats that are mostly unilateral
2	Serial (≥3 times s^{-1}) but irregular contractions
1	Sporadic contractions (<3 times s^{-1}) only
0	No movements during the 5 min observation time

Analysis of durations and intervals of tail-beating bursts by whole larvae

We intended to examine the periodicity of the movements expressed by unfragmented whole larvae. We utilized MC to increase the viscosity of the medium (ASW) for swimming whole larvae in order to limit the amount of displacement by swimming and restrict

Journal of Experimental Biology (2022) 225, jeb243828. doi:10.1242/jeb.243828

otherwise variable sensory inputs (accidental collision with the dish bottom/wall or water surface as well as changes in the body direction to illuminated light, which are associated with free swimming within a dish). A few hatched larvae (19–20 hpf) were transferred into ASW containing 1% MC and the medium was mixed well. After allowing 10 min for acclimation to the viscous medium, we recorded movements expressed by the larvae for 15–20 min using the stereomicroscope and video camera as described above. 'Swimming' bursts with regular bilateral tail beats (well-patterned movements) were used to evaluate the durations and intervals of bursts, while sporadic contractions of the tail, including flick-like movements, were disregarded.

To estimate the artificial effects of increases in the viscosity of the water medium on the expression of movements, we compared tail-beating frequencies in swimming bursts by whole larvae in ASW containing 0% (ASW alone), 0.5%, 1% or 2% MC. To calculate tail-beating frequency, we placed several larvae (~24 hpf) in ASW or ASW containing 0.5%, 1% or 2% MC and then mixed the solution well. The swimming-like bursts of tail beats were recorded using the high-speed camera as described above (VCC-H1000, Digimo) mounted on the stereomicroscope (MZIII, Leica) at 250 frames s^{-1}. As the first and last beating cycles in a series of tail beats (a burst) were often irregular, we calculated the frequency of tail beating from the duration of five tail-beating cycles excluding the first and last cycles. The light condition was kept constant among the different MC conditions. All data obtained were analyzed using Microsoft Excel and R (v.3.5.0). Movie files were prepared using ImageJ, Video Editor on a Windows 10 PC, and iMovie on an iPad Pro.

Statistical analysis of time-series data

To evaluate the periodicity of tail-beating bursts expressed by fragmented or whole *Ciona* larvae, we quantified the extent of deviations of the burst durations and intervals from a Poisson random process. Poisson random processes are used as mathematical models of natural events that occur in time (e.g. Durrett, 2012). The distribution patterns of intervals of Poisson random processes are known to be on a negative exponential curve $\lambda e - \lambda t$, where the time constant $\tau\,(=\lambda^{-1})$ represents the mean value of intervals.

To quantify the extent of deviations, we introduced the concept of the 'zero-mean normalized cross-correlation criterion', which is commonly utilized to measure similarities between images in the field of digital image processing (e.g. Pan, 2011). For each dataset, the frequency of a histogram is represented as a sequence $f_1, f_2, \ldots, f_{30}$, where we set bin intervals from 0 to 60 s with 2 s increments and from 0 to 15 s with 0.5 s increments for the intervals and durations of tail-beating bursts, respectively. For each dataset, we considered the Poisson distribution with the same mean value, and we made its histogram with the same bin intervals. The frequency is represented as another sequence $g_1, g_2, \ldots, g_{30}$. The zero-mean normalized cross-correlation (simply referred to as cross-correlation, CC, in the present study) of these two sequences, f_i and g_i, is defined by the following equation (Pan, 2011):

$$\mathrm{CC} = \frac{\sum_{i=1}^{m} \bar{f}_i \bar{g}_i}{\sqrt{\left(\sum_{i=1}^{m} \bar{f}_i^2\right)\left(\sum_{i=1}^{m} \bar{g}_i^2\right)}}, \quad (1)$$

where

$$\bar{f}_i = f_i - \frac{1}{m}\sum_{j=1}^{m} f_j, \quad (2)$$

$$\bar{g}_i = g_i - \frac{1}{m}\sum_{j=1}^{m} g_j \quad (3)$$

and m is 30, which denotes the number of bins.

In this criterion, when a CC value is close to 1, 0 or −1, the two histograms are considered to be similar, dissimilar or inversely correlated, respectively. The CC value between a uniform distribution with a mean interval of 20 s and a Poisson distribution with a mean interval of 20 s was 0.64. We regarded time-series data with CC values <0.3 to sufficiently deviate from a Poisson random process, and those with CC values >0.75 to be close to a Poisson random process.

RESULTS

Experimental identification of the body region that autonomously expresses tail-beating bursts

By segmenting *Ciona* larval bodies at various positions, we investigated whether the anterior and posterior fragments expressed well-patterned alternating tail beats (Fig. 1). Segmentation sites were represented as a relative location (%) along the longitudinal axis of the body, in which the positions of the trunk–tail junction and tail tip were defined as 0% and 100%, respectively (see also Materials and Methods). Anterior fragments showed no movement when cut sites were located within the trunk (represented by negative values) [Fig. 1A; MI=0, 19 cases in 19 trials (19/19)]. This is consistent with the fact that the trunk of *Ciona* larvae harbors no machinery for bending (e.g. Katz, 1983; Bone, 1992). The truncated tail that remained in the anterior fragments clearly exhibited alternating beats when cut sites were located posterior to 5.7% (Fig. 1A; Movie 1; MI=4, 100/100). However, anterior fragments showed no movement when the remaining tail was shorter than 5.7% (Fig. 1A; MI=0, 6/6). These results suggest that the proximal 5.7% portion of the tail in combination with the trunk is necessary and sufficient to express alternating tail beats, while the distal 5.7–100% of the tail is not required.

Posterior fragments did not show evident movements when cut sites were located posterior to 55% (Fig. 1B; MI=0, 22/23). Posterior fragments exhibited sporadic and irregular movements with a higher frequency (≥3 Hz; Movie 1; MI=2, 33/84) or lower frequency (<3 Hz, MI=1, 47/84) when the cut sites were in 0–55%. The majority of movements observed were neither regularly rhythmic nor left–right alternating (only one exception in 84 trials, in which the cut site was very close to the trunk–tail junction) (Fig. 1B). In contrast, when cut sites were in the trunk, posterior fragments exhibited rhythmic and alternating tail beating (Fig. 1B; Movie 1; MI=4, 18/19). This result demonstrated that the anterior portion of the trunk was not necessary to express reciprocal tail beating. As a posterior fragment cut at −6.7% was the only case in which tail beating was not rhythmic, we concluded that a posterior fragment with a short posterior portion of the trunk (range −6.7–0% region, as the largest estimation) sufficiently expressed alternating tail beats. Furthermore, body parts comprising the tail region only did not express reciprocal tail beating (105/106 cases); therefore, a small portion of the posterior trunk (−6.7% or shorter) was required for the expression of rhythmic reciprocal tail beating. Based on these results, we concluded that the body part spanning −6.7–5.7% represented a necessary and sufficient region, as the largest estimation, for expressing reciprocal tail beating in *Ciona* larvae.

It is important to note that these results were obtained from body fragments placed in ASW only, i.e. without any additional stimuli.

Journal of Experimental Biology (2022) 225, jeb243828. doi:10.1242/jeb.243828

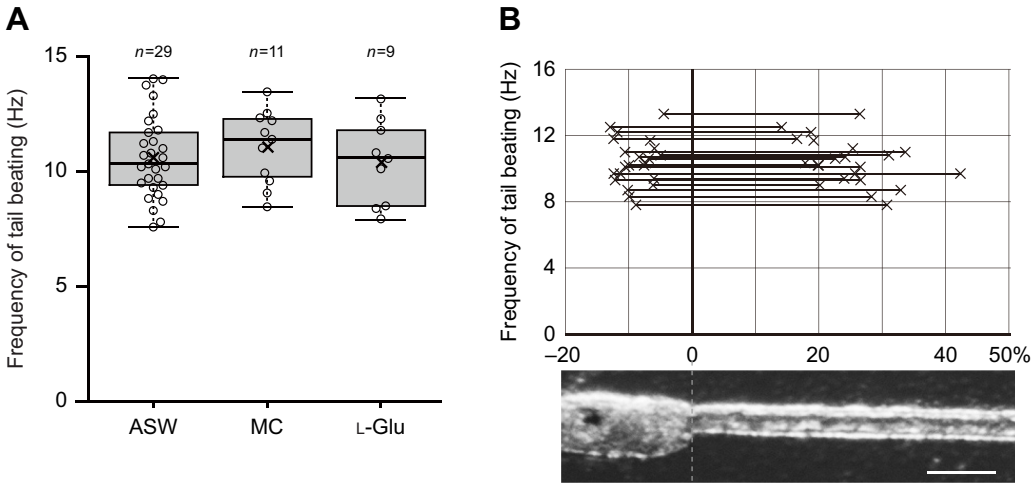

Fig. 2. Frequency of tail beating in 'mid-piece' fragments of *Ciona* larvae. (A) Frequency of tail beating exhibited by mid-piece fragments in artificial seawater (ASW) and in the presence of methylcellulose (1% MC in ASW) or L-glutamate (100 µmol l^{-1} L-Glu in ASW). *n* denotes the number of fragments examined. (B) Mid-piece fragments (*n*=22) from which the anterior trunk and posterior tail were excluded showed tail beating at a frequency of 8–13 Hz. Cut sites (marked by a cross) are indicated along the horizontal axis, which is defined as 0% and 100% at the trunk–tail junction and tail tip, respectively. Horizontal bars between pairs of crosses indicate the remaining portion of the body in mid-piece fragments. An image of a *Ciona* larva is shown for reference. Scale bar: 100 µm.

Nishino et al. (2010) previously reported that the swimming movements of *Ciona* larvae, from which a large anterior portion of the trunk had been removed, were activated by the addition of the excitatory amino acid L-Glu. However, the present results demonstrated that locomotor output in decapitated *Ciona* larvae was sufficiently driven without any activator agonists. To resolve this contradiction and carefully examine the potential activation effect(s) of L-Glu on the movements of body fragments, e.g. posterior fragments cut posteriorly to 5.7%, we performed another series of experiments using ASW containing 100 µmol l^{-1} L-Glu. The results obtained showed that the relationships between cut sites and movement patterns in the presence of L-Glu did not markedly differ from those without L-Glu (Fig. S1; cf. Fig. 1).

Mid-piece fragments sufficiently express alternating tail beats

The results presented above suggest that the middle part of the larval body including the trunk–tail junction (herein called the mid-piece), spanning −6.7–5.7% as the longest estimation, represents a necessary and sufficient region to express rhythmic reciprocal tail beating. Mid-piece preparations that lacked most of the anterior part of the trunk and most of the posterior tail clearly expressed alternating tail beats (Movie 2; MI=4, −6.5–19.2% mid-piece in the indicated case). We investigated quantitative relationships between the remaining part/length of mid-piece fragments and the frequency of alternating tail beats using the high-speed camera. This quantitative analysis revealed that the mid-piece fragments generated alternating tail beats of 10.6±1.8 Hz (*n*=29) (Fig. 2A), which did not appear to be related to the part of the body that remained or the length of the remaining fragment (*n*=22) (Fig. 2B). Increases in the viscosity of circumferential fluid using 1% MC did not significantly affect the frequency of tail beating (11.1±1.6 Hz, *n*=11; $P>0.3$, Student's *t*-test, two-tailed). We examined the effects of L-Glu (100 µmol l^{-1}) on the frequency of tail beating expressed by mid-piece fragments, and found no significant difference from that by untreated mid-piece fragments (10.4±1.8 Hz in 100 µmol l^{-1} L-Glu, *n*=9; $P>0.3$, Student's *t*-test, two-tailed). Furthermore, dose-dependent increases were not observed in tail-beating activities, the average duration of tail-beating bursts or cumulative duration of bursts per minute in ASW containing 0, 100 µmol l^{-1} or 1 mmol l^{-1} L-Glu (Fig. S2; $P>0.05$ in every combination, Student's *t*-test, two-tailed).

The mid-piece of *Ciona* larva exhibits the periodicity of patterned tail beating

In the course of examinations on mid-piece fragments, we noted that these fragments expressed bursts at approximately 20 s intervals, i.e. with an almost regular periodicity (Fig. 3; Movie 3). We segmented 22–24 hpf swimming larvae to isolate mid-piece fragments and measured the length of time from the beginning of one burst event to that of the next.

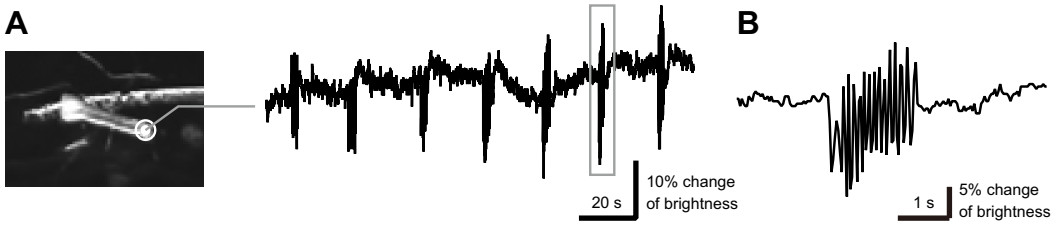

Fig. 3. Periodicity of tail-beating bursts expressed by mid-piece fragments. (A) A point of interest (double circle) was set on the posterior tip of a mid-piece fragment (left). Brightness changes at that point reflect alternating tail beats (right). Fluctuations in the baseline reflect subtle changes in the position of the fragment as well as noise in a series of images, but not beating of the tail. (B) Magnified trace of a tail-beating burst (indicated by the rectangle in A). Alternating tail beats of ~10 Hz were detected on the trace.

Journal of Experimental Biology (2022) 225, jeb243828. doi:10.1242/jeb.243828

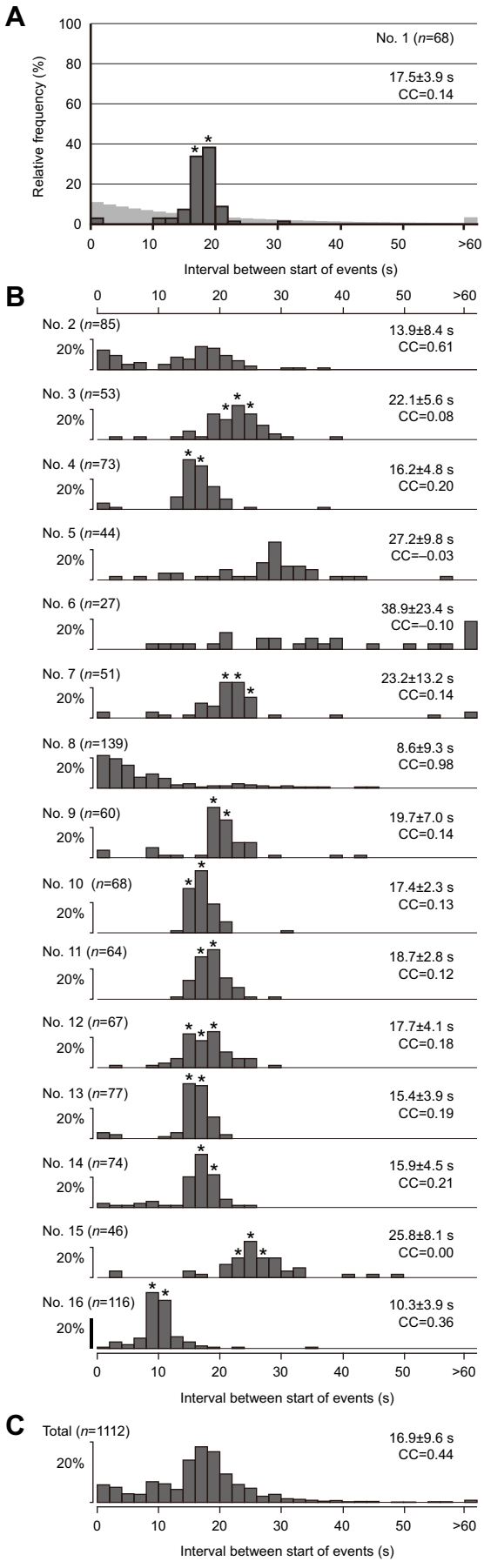

Fig. 4. Cycle periods of tail-beating bursts exhibited by mid-piece fragments. (A) A histogram showing cycle periods of tail-beating bursts expressed by a mid-piece fragment (no. 1, approximately 20 min after cutting) from the start time of one burst to the start time of the next burst (dark gray). Relative frequencies of the lengths of cycle periods in n=68 cycles, Mean±s.d. values and the CC (cross-correlation) value are shown. Light gray bars are a reference to show the distribution pattern of relative frequencies when the occurrence of bursts follows a Poisson random process in which events randomly occur at a constant average rate (17.5 s in this case). (B) Histograms showing the cycle periods of tail-beating bursts expressed by 15 other mid-piece fragments (nos 2–16) (dark gray bars). (C) A histogram of aggregated data from individual mid-piece fragments (nos 1–16). n denotes the number of examined cycle periods of tail-beating bursts. Mean±s.d. values for cycle period length in each fragment are shown. Vertical ticked axes represent 20% of the relative frequency. Asterisks indicate the neighboring top 2 or 3 ranks with the peak at 8–26 s, which include ≥50% of the samples. CC values indicate the extent to which the distribution of data differs from the Poisson distribution (see Materials and Methods).

Stochastic processes, such as Poisson random processes, are useful for modeling natural phenomena that appear to occur in a random manner (e.g. Durrett, 2012). In a Poisson process, the distribution of time intervals between events is expected to be on a negative exponential curve ($\lambda e^{-\lambda}t$), where the time constant ($=\lambda^{-1}=\tau$) corresponds to the mean value of intervals and also to the standard deviation (s.d.). Therefore, if tail-beating bursts expressed by mid-piece fragments occur randomly following a Poisson process, a histogram of intervals may be close to the negative exponential distribution with a time constant of ∼20 s. In contrast, the present results clearly showed intervals of ∼20 s between bursts (Fig. 4; in 13/16 cases, CC values <0.3, see Materials and Methods; in 12/16 cases, ≥50% of events were included in the neighboring top 2 or 3 ranks with the peak at 8–26 s, marked with asterisks). The distribution pattern of intervals differed markedly from the negative exponential pattern [Fig. 4A; cf. histograms of intervals between start–start timings of tail-beating bursts expressed by a mid-piece fragment, where τ=17.5 s (dark gray), and of intervals of stochastically occurring events (calculated, light gray)]. There was only one case (1/15) that showed a negative exponential pattern with the mean value being close to the s.d. value (Fig. 4B, no. 8; CC=0.98).

To estimate the stability of periodic tail-beating bursts, fragments were left for 1.5 h or longer before examining the timing of bursts. We prepared mid-piece fragments derived from 22–24 hpf larvae, left them for 1.5–3.5 h, and then measured the durations and intervals of tail-beating bursts (ignoring sporadic flick-like twitches) (Fig. 5A,B). To examine the temporal patterns of tail-beating bursts in more detail, we measured the duration (start–end) and interval (end–start) of bursting events in subsequent analyses, not the length of time between neighboring start–start timings as shown above. The results obtained revealed that the periodic expression of tail beating was retained even 1.5–3.5 h after cutting (Fig. 5A,B; in 16/17 cases, CC values of intervals <0.3; in 13/17 cases, ≥50% of intervals were included in the neighboring top 2 or 3 ranks with the peak at 10–30 s, marked with asterisks in Fig. 5B), and the duration and interval of tail-beating bursts were estimated to be 2.4±1.9 s and 19.8±8.4 s, respectively (mean ±s.d.; N=17 individuals, n=866 events). This estimation showed that the cycle period became slightly longer than that immediately after cutting (cf. Figs 4 and 5A,B). This periodic pattern was also observed for mid-piece fragments derived from earlier larvae (19–20 hpf) (Fig. S3; in 17/17 cases, CC values of intervals <0.3; in 13/17 cases, ≥50% of intervals were included in the neighboring top 1–3 ranks with the peak at 10–30 s, marked with asterisks in Fig. S3B),

Journal of Experimental Biology (2022) 225, jeb243828. doi:10.1242/jeb.243828

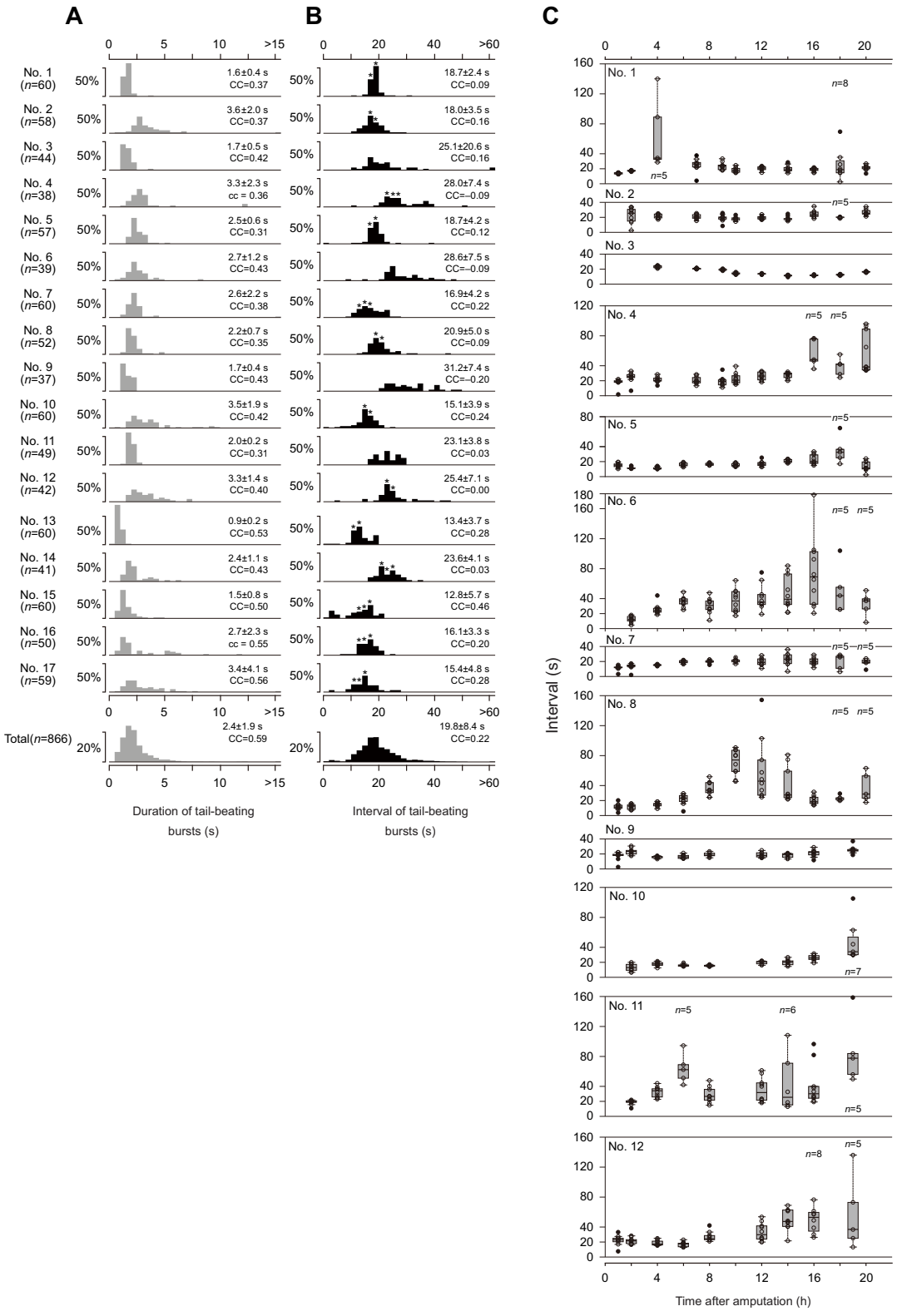

Fig. 5. Stability of cycle periods of tail-beating bursts expressed by mid-piece fragments. (A,B) Histograms showing the durations (A) or intervals (B) of tail-beating bursts expressed by mid-piece fragments (nos 1–17; 1.5 h after cutting at 22–24 hours post-fertilization, hpf). Histograms of aggregated data from individual mid-piece fragments are shown at the bottom ('Total'). *n* denotes the number of examined cycle periods of tail-beating bursts in each specimen. Mean ±s.d. values of the durations and intervals of each fragment are shown. Vertical ticked axes represent 50% (or 20% for the total histograms) of the relative frequency. Asterisks indicate the neighboring top 2 or 3 ranks with the peak at 10–30 s, which include ≥50% of samples. CC values indicate the extent to which the distribution of data differs from the Poisson distribution. (C) An approximately 20 s interval of tail-beating bursts is maintained for half a day or longer. Intervals between ≤11 consecutive bursts expressed by mid-piece fragments (nos 1–12) were measured every 0.5–2.0 h up to 20 h after cutting at 22–24 hpf. Open circles indicate data utilized for box plots, and filled circles are outliers. *n* represents the number of measured intervals; only *n* values <10 are indicated above or below the box plots.

Journal of Experimental Biology (2022) 225, jeb243828. doi:10.1242/jeb.243828

in which the duration and interval of tail-beating bursts were 2.8 ±3.0 s and 21.0±8.1 s, respectively (N=17, n=781).

We also measured the intervals of tail-beating bursts up to 20 h after cutting at 22–24 hpf, and found that the majority of prepared mid-piece fragments continued to show periodicity for 12 h or longer (Fig. 5C). These results demonstrated that the mid-piece region of the *Ciona* larval body expresses an intrinsic, autonomous and robust rhythm to generate ∼2.5 s tail-beating bursts at ∼20 s intervals.

Periodicity of swimming events in unfragmented larvae

We investigated how the periodicity observed for mid-piece fragments was related to swimming patterns expressed by the whole bodies of *Ciona* larvae. We considered it difficult to trace the temporal pattern of a single larva that freely swims in seawater and also to exclude variable sensory stimulation, such as uncontrolled physical contact with the water surface. Therefore, we placed a larva in seawater containing MC to limit its translocation and prevent uncontrolled sensory stimulation as much as possible.

Using the high-speed camera, we confirmed that the frequency of tail beats did not markedly differ among larvae (∼24 hpf) in ASW with 0%, 0.5%, 1% and 2% MC, whereas statistical tests indicated that it was significantly lower in 2% MC (Fig. S4; P≈0.04, one-way ANOVA; P<0.05 between 0% and 2% MC only, Tukey's test). This analysis revealed that the addition of ≤1% MC and the accompanying increase in viscosity did not markedly affect swimming performance. It also showed that the whole body of larvae exhibited a higher frequency of tail beats (15–20 Hz) than mid-piece fragments (8–13 Hz) (cf. Fig. 2 and Fig. S4).

We observed unfragmented larvae (19–20 hpf) in the presence of 1% MC and measured the durations and intervals of tail-beating bursts. The durations of patterned tail beating varied markedly, but their intervals were not along a negative exponential curve, which implied that the occurrence of tail-beating bursts did not follow a Poisson random process (Fig. 6A,B; in 7/17 cases, CC values in intervals <0.3, see Materials and Methods; in 9/17 cases, ≥50% of intervals were included in the neighboring top 2 or 3 ranks with the peak at 8–26 s, marked with asterisks in Fig. 6B). The mean interval between swimming bursts was shorter than 20 s (Fig. 6B,E; 15.0±9.5 s, N=17, n=567). We utilized an optical filter (high-pass 590 nm) to eliminate the light visible to *Ciona* larvae (Nakagawa et al., 1999; Nishino et al., 2011), and noted that the interval time became shorter (Fig. 6D,E; 10.4±7.4 s, N=10, n=810) and slightly more periodic [variance in the dark=54.2 (n=810) versus variance in the light=90.3 (n=567); P<10^{-20}, Mann–Whitney–Wilcoxon test]. On the other hand variation in the duration of bursts by whole larvae placed in the light was markedly higher than that by mid-piece fragments [Fig. 6E; variance for whole larvae in the light=168.9 (n=567) versus variance for mid-piece fragments=9.2 (n=781)], suggesting that variable inputs, which are derived through the BV and other sensory systems into the mid-piece, shortened or lengthened swimming duration (Fig. 6A,E). The distribution patterns of the durations of tail-beating bursts under light and dark conditions were very similar to the negative exponential distributions predicted by Poisson random processes (Fig. 6E; CC=0.82 and 0.78, respectively). These results suggest that *Ciona* larvae have a non-stochastic, but variable temporal pattern in the intervals of swimming bursts and that larvae modify periodicity for swimming intervals and durations accommodated to sensory inputs that are processed in parts other than the mid-piece.

DISCUSSION

The *Ciona* larval body region around the trunk–tail junction is necessary and sufficient for the autonomous expression of alternating tail beats

In the present study, we identified the body region that is required and sufficient for the expression of alternating tail-beating bursts. This body region includes a short part of the posterior trunk and approximately 6% of the anterior portion of the tail, representing one-tenth or less of the length of the ∼1 mm whole body.

The results obtained herein demonstrated that the trunk region, excluding the most posterior portion, was not required to generate patterned movements, although it was unclear whether the anterior trunk was sufficient. The posterior region of the tail was neither necessary nor sufficient for the expression of patterned movements, even in the presence of the activation amino acid, L-Glu. Short posterior fragments (segmented at 55–100%) did not show any movement, while longer posterior fragments of the tail (segmented at 3–55%) exhibited irregular movements. As muscle cells occupy up to ∼85% of the length of a *Ciona* larval tail (see Nishino et al., 2011), it was reasonable that posterior fragments did not move when cut sites were located posterior to 85% of the tail length.

The present results showed that posterior fragments did not move when cut sites were in the 55–85% region, whereas they moved in most cases when cut sites were at 0–55%. The reason for these results warrants further study. One possibility is that MTNs, which are sparsely distributed along the CNC and express the cholinergic neuron marker (Imai and Meinertzhagen, 2007; Horie et al., 2010; Ryan et al., 2016), are present in longer, but not in shorter posterior fragments. As larval muscle cells are activated by cholinergic inputs (Ohmori and Sasaki, 1977; Nishino et al., 2011), MTNs may constitute a group of motor neurons, and their spontaneous excitation may underlie the flick-like, sporadic movements of longer posterior tail fragments. Indeed, longer tail fragments moved more frequently (Fig. 1B). Two pairs of bipolar tail neurons (BTNs), a type of peripheral neuron, have also been shown to reside in the middle of the tail (Coric et al., 2008; Stolfi et al., 2015). Anterior and posterior pairs of BTNs express markers for the inhibitory neurotransmitter GABA and the excitatory neurotransmitter acetylcholine, respectively (Zega et al., 2008; Stolfi et al., 2015; Kim et al., 2020). The spontaneous firing of the posterior pair of BTNs may also lead to sporadic movements of posterior tail fragments.

Anterior fragments expressed alternating tail beats when they contained at least 5.7% of the proximal portion of the tail. Two pairs of contralateral inhibitory neurons called ACINs have been identified in this proximal tail region (Horie et al., 2010; see also Nishino et al., 2010). The present results provide direct evidence for the essential role of ACINs in the generation of alternating tail beats, which has long been proposed (Horie et al., 2010; Nishino et al., 2010). According to a previous study, the anterior pair of ACINs, at least, appears to be included in the proximal 5% of a *Ciona* larval tail (see Horie et al., 2010). In the present study, we originally assumed the possible occurrence of unilateral rhythmic movements in some fragments (MI=3, Table 1). However, all of the rhythmic movements observed were alternating, with no examples of unilateral beating (MI=3) in our trials (>200). These results support the inhibitory interaction between the left and right halves through the ACIN pairs enabling reciprocal movements.

However, the reason why the removal of most of the posterior tail (cutting at 0–5.7%), i.e. the total elimination of ACINs, led to the complete loss of movements, but not to the irregularity of movements, remains unknown. One simple explanation is a

Journal of Experimental Biology (2022) 225, jeb243828. doi:10.1242/jeb.243828

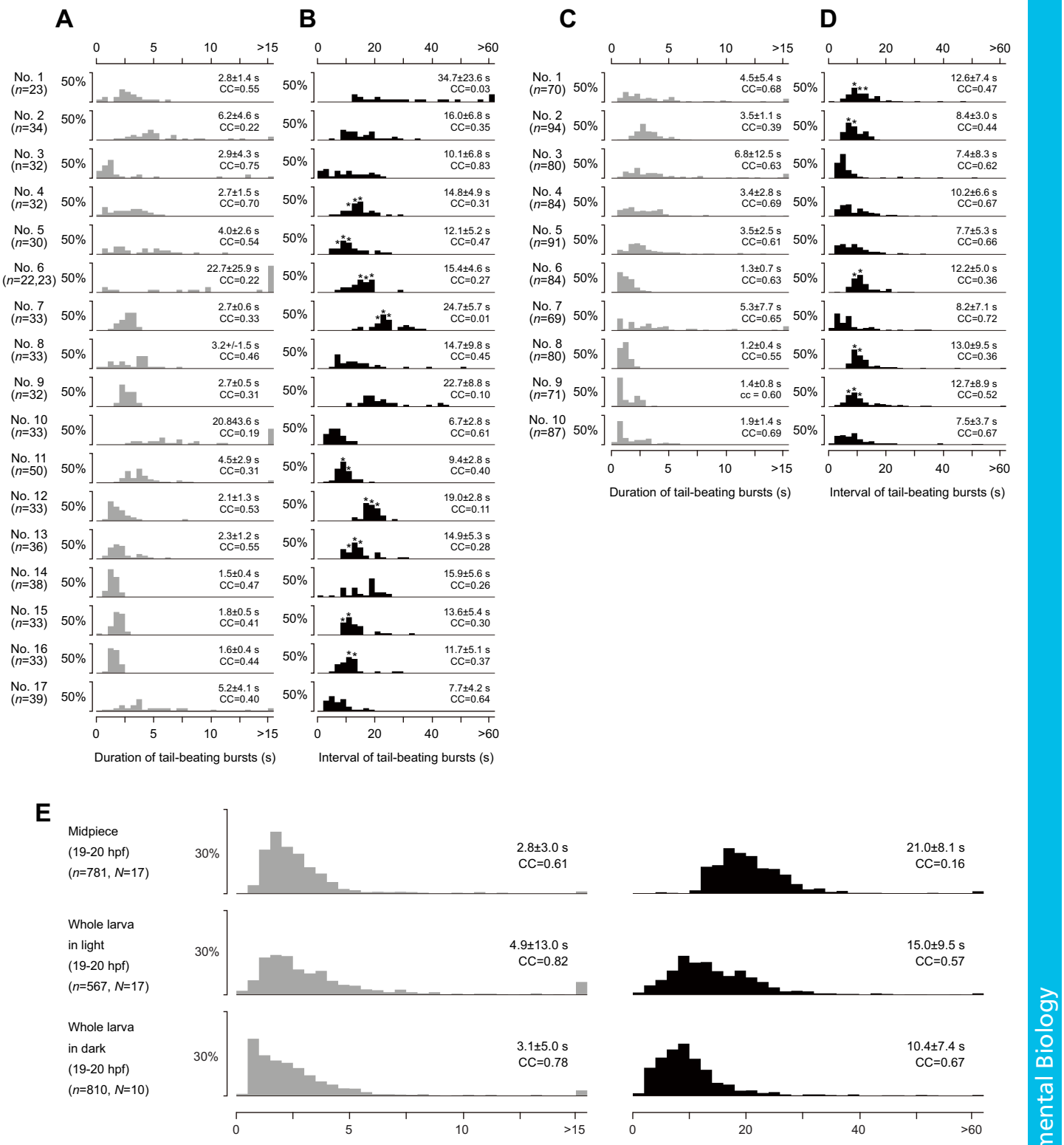

Fig. 6. Temporal patterns of tail-beating bursts expressed by unsegmented whole larvae under light and dark conditions. (A–D) Histograms showing the durations (A,C) or intervals (B,D) of tail-beating bursts expressed by unsegmented whole larvae (19–20 hpf) placed in 1% MC under light (A,B; nos 1–17) or dark (C, D; nos 1–10) conditions. *n* denotes the number of examined cycle periods of tail-beating bursts in each specimen. Mean±s.d. values of the durations and intervals of each fragment are shown. Vertical ticked axes represent 50% of the relative frequency. Asterisks indicate the neighboring top 2 or 3 ranks with the peak at 8–26 s, which include ≥50% of samples. CC values indicate the extent to which the distribution of data differs from the Poisson distribution. (E) Histograms of aggregated data from different conditions. Relative frequencies of the durations (left, gray bars) and intervals (right, black bars) of tail-beating bursts expressed by mid-piece fragments prepared at 19–20 hpf (top, *N*=17; individuals examined corresponding to the data shown in Fig. S2A,B), whole larvae (19–20 hpf) placed under light conditions (middle, *N*=17; corresponding to those shown in A,B) and whole larvae (19–20 hpf) placed under dark conditions (bottom, *N*=10; corresponding to those shown in C,D) are shown. *n* denotes the summed number of cycle periods. Mean±s.d. values of the durations and intervals are shown. Vertical ticked axes represent 30% of the relative frequency.

Journal of Experimental Biology (2022) 225, jeb243828. doi:10.1242/jeb.243828

physical limitation; namely, that the movement of fragments with very short portions of the tail was not detectable by eye. Another possibility is irreparable damage to motor endplates that are crucial for the expression of tail beating because the frondose terminals of a major pair of motor neurons, called MN1, attach anterior muscle cells at the level at which ACINs reside (Ryan et al., 2016).

By referring to the connectome analyses conducted by Ryan et al. (2016, 2017, 2018), we estimated that the mid-piece region contained 25 neurons, at most, in the MG and 1 or 2 pairs of ACINs posteriorly associated with the MG (27–29 neurons in total) in the CNS. Five pairs of motor neurons that extend axons posteriorly along the CNC have been identified in the MG, which is located around the trunk–tail junction (Katz, 1983; Ryan et al., 2016; 2017; Kawai et al., 2021). Based on our results showing that a small portion of the posterior trunk sufficiently conferred the ability to express patterned movements (Fig. 1B), a posterior portion of the MG containing some, but not all, posterior pairs of motor neurons and ACINs (several neurons in total) may constitute a sufficient circuit (Fig. 7, darker area).

The CPG comprises, by definition, neural circuits in the CNS that generate a stereotypical motor pattern without any sensory inputs or proprioceptive feedback (Bässler, 1986; Delcomyn, 1980; 1998). Based on this meaning, it may still be premature to claim that our mid-piece preparation represents a CPG that is free of sensory inputs. By cutting off large portions of the anterior trunk as well as the posterior tail, most of the sensory neurons that have been identified to date, including papillar neurons, most of the epidermal sensory neurons (ENs), and BTNs were excluded; however, some ENs, including pACENs, DCENs and VCENs (Yokoyama et al., 2014; Ryan et al., 2018), may have remained in our mid-piece preparations. Afferents from ENs are concentrated in the posterior part of the BV, e.g. eminens cells (Horie et al., 2008a; Ryan et al., 2018), and other dense innervations have also been found in the dorsal area of the MG, at which ascending MG interneurons, AMG neurons, reside (Ryan et al., 2018). Although ENs generally express a marker for glutamatergic neurons (Horie et al., 2008a), the L-Glu treatment did not change the movement patterns of mid-piece fragments in the present study. Furthermore, a change in the viscosity of circumferential fluid did not markedly affect tail beating, although ENs are considered to be mechanosensory. These results imply that inputs from ENs did not have an impact on the generation of locomotion patterns in mid-piece fragments.

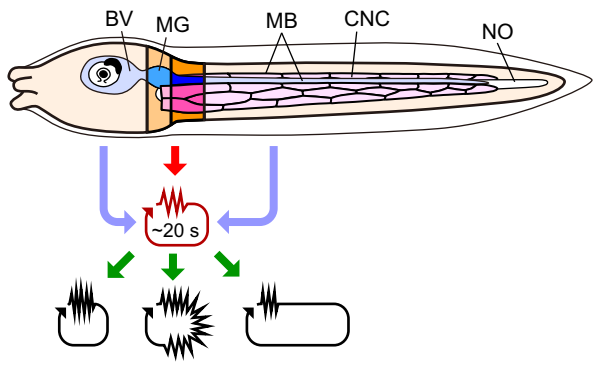

Fig. 7. A proposed model for the expression of swimming performance by *Ciona* larvae. The region with dark colors indicates the required 'mid-piece' part for expressing autonomous reciprocal tail beating. The lighter part of this region indicates the largest estimation, and the darker part highlights the predicted smallest region that harbors the potential to autonomously output tail-beating bursts with a ~20 s cycle period (red arrow). Other regions possessing various sensory apparatus, such as photoreceptors and a gravity sensor (represented by pigments in the BV), modify this endogenous and autonomous drive to form swimming performance (blue and green arrows), which is accommodated to sensory inputs. BV, brain vesicle; CNC, caudal nerve cord; MB, muscle band; MG, motor ganglion; NO, notochord.

The mid-piece of the *Ciona* larva expresses an autonomous cycle period of tail-beating bursts

The mechanism by which the neuronal network in the posterior MG and ACINs autonomously expresses alternating tail beats with a ~20 s cycle period is of interest. Neural circuits for expressing 'autonomous and periodic' bursts have been found in mammalian brain slice preparations, such as medullary preBötzinger and Bötzinger complexes for breathing rhythm formation (Smith et al., 1991; Koshiya and Smith, 1999; Ghali, 2019). Although anesthetization slows respiration rhythms, rhythmic respiration is maintained at a 'basal' level. Therefore, the basal rhythm for breathing is autonomous in these complexes, and may be up-regulated by various modifiers, such as involuntary homeostatic feedback (including the concentration of O_2 and body temperature) and intentional controls (such as sighing). These characteristics of the mammalian medullary complexes are similar to those of the system in the mid-piece fragment of *Ciona* larvae. The mid-piece fragments expressed slower tail beating and longer (but more periodic) intervals between their bursts, representing a basal status, and this basal rhythm was up-regulated (i.e. the tail-beat frequency was increased and burst intervals shortened) by inputs from other parts.

The present results did not reveal the types of elements in the mid-piece fragment generating the autonomous rhythm or the underlying mechanisms. Akahoshi et al. (2017) examined the firing patterns of embryonic cells, including differentiating neurons, using a fluorescent Ca^{2+} indicator, and recently demonstrated that a pair of cholinergic motor neurons at the posterior MG, called A10.64 or MN2 (see also Ryan et al., 2016; Navarrete and Levine, 2016), autonomously increased the intracellular concentration of Ca^{2+} that corresponded to tail beating at ~20 s intervals in the late tailbud stage (Akahoshi et al., 2021). The oscillatory rhythm of Ca^{2+} transients that they found in the posterior MG corresponds well with the rhythm of tail-beating bursts found in our mid-piece preparations; therefore, the MN2 pair may be an origin of the swimming rhythm.

Body regions outside the mid-piece modify the autonomous activity of the mid-piece

Ascidian larvae intermittently execute tail-beating bursts to swim, and larvae gravitate downward during intervals. As larvae exhibit negative gravitaxis (Svane and Young, 1989; Tsuda et al., 2003a; Bostwick et al., 2020), the temporal control of the durations and intervals of larval tail beating represents a crucial strategy for sessile ascidians to disperse progeny. The duration of tail-beating bursts was previously reported to be under the control of neurotransmission (Brown et al., 2005). Based on the present results, we propose that swimming performance expressed by the whole *Ciona* larva is represented by modifications to a slower basal rhythm intrinsic to the mid-piece region via inputs from other parts of the body (Fig. 7). This provides a mechanistic basis for the temporal control of swimming performance in *Ciona* larvae (Fig. 7).

Recent advances in big-data analysis of the swimming trajectories and body postures of moving *Ciona* larvae by machine vision and automated parameterization algorithms have led to the categorization of their motor behaviors (Rudolf et al.,

2019; Athira et al., 2021 preprint). This repertoire of swimming behaviors may be viewed as patterns of modifications from the nervous system in the BV and posterior CNC to that in the MG and anterior CNC.

Body regions outside the mid-piece increased variation in the duration of swimming bursts and shortened the intervals of bursts. Moreover, in larvae with the BV placed under dark conditions, swimming intervals were further shortened. Regarding neural signals descending from photoreceptors in the BV to MG neurons, excitatory and inhibitory visuomotor pathways have both been indicated (Kourakis et al., 2019; Bostwick et al., 2020). The results shown in Fig. 6 reflect enhanced excitatory and/or suppressed inhibitory visuomotor signals under constant dark conditions (Kourakis et al., 2019). The unsegmented larvae used in the present study were young (19–20 hpf). *Ciona* larvae gradually develop, for example, the ability to respond to light stimuli (Kajiwara and Yoshida, 1985; Tsuda et al., 2003b; Zega et al., 2006; Horie et al., 2008b; Salas et al., 2018). The use of larvae at different developmental times may have revealed different patterns of modifications to the mid-piece, the properties of which are relatively constant.

Phylogenetic implications of systems for the expression of swimming locomotion

Ascidian larvae share tadpole-shaped bodyplans with vertebrates. Common features are also indicated in their system for the alternation of left–right outputs, in which ipsilaterally projecting excitatory interneurons/motoneurons and inhibitory commissural interneurons are coupled between the left and right sides (Roberts et al., 2010; Horie et al., 2010; Nishino et al., 2010; Ryan et al., 2017; Grillner and El Manira, 2020). Furthermore, fictive swimming in vertebrate spinal cords driven by the bath application of excitatory amino acid analogs, such as *N*-methyl-D-aspartate, showed periodic cycles of the duration and interval of bursts (Grillner, 1975; Cangiano and Grillner, 2003; Wiggin et al., 2012), similar to periodic tail-beating bursts by the mid-piece fragment of *Ciona* larvae. It is important to note that the hyperpolarization-activated current, which is known to play crucial roles in generating rhythms in various systems (Maylie and Morad, 1984; Angstadt and Calabrese, 1989; Kiehn et al., 2000; Thoby-Brisson et al., 2000; Harris-Warrick and Johnson, 2010), is strongly expressed in a type of excitatory interneuron in the spinal cord of frog tadpoles and is involved in the generation of locomotor rhythms (Picton et al., 2018).

The present results also revealed several significant differences between the ascidian larva and vertebrate swimmers. The system in the *Ciona* larva is localized and autonomously expresses outputs, while the CPG neuronal circuits of vertebrate fish and tadpoles are ubiquitously distributed along the spinal cord and are silent without an activating signal (e.g. Roberts, 2000; Wiggin et al., 2012; Grillner and El Manira, 2020). As indicated above, the mid-piece of *Ciona* larvae has several characteristics reminiscent of those of the breathing rhythm centers in the mammalian brain. These systems are both based on an autonomous, involuntary and slower rhythm of bursts that secures the basal level of locomotion. This basic activity is modified by several lines of inputs. These modifications allow larvae to swim in an *ad hoc* manner in response to various sensory stimuli.

Animals often express locomotion periodically; even jellyfish have a rhythm of pulsation and also have periods for bursting and resting (e.g. Anderson, 1979). The present results demonstrated that the exclusion of BV, posterior CNC and associated sensory systems unmasked the basal rhythms for locomotion of *Ciona* larvae. This element in the trunk–tail junctional region of *Ciona* larvae may represent one of the simplest systems for animal locomotion and warrants further study in identifiable cells (Ryan et al., 2016; Nishino, 2018; Gibboney et al., 2020; Akahoshi et al., 2021).

Acknowledgements

We thank Drs Satoe Aratake, Megumi Kotsuka, Akihiro Yoshikawa, Makoto Nozawa and Manabu Yoshida (Misaki Marine Biological Station, The University of Tokyo), Drs Reiko Yoshida, Chikako Imaizumi and Yutaka Satou (Laboratory of Developmental Genomics, Department of Zoology, Graduate School of Science, Kyoto University), and other staff who distribute *Ciona* under the National BioResource Project, AMED, Japan. We are grateful to Dr Kohji Hotta (Keio University) for his discussions and for kindly sharing unpublished data. We sincerely thank Dr Yasushi Okamura and Dr Ian A. Meinertzhagen for their encouragement and critical reading of the manuscript. We also appreciate the valuable comments by the anonymous reviewers, which markedly improved the quality of the manuscript.

Competing interests

The authors declare no competing or financial interests.

Author contributions

Conceptualization: T.H., A.S.N.; Methodology: T.H., S.H., Y.I., A.S.N.; Software: Y.I.; Validation: T.H., S.H., Y.I., A.S.N.; Formal analysis: T.H., S.H., Y.I., A.S.N.; Investigation: T.H., S.H., A.S.N.; Data curation: T.H., S.H., Y.I., A.S.N.; Writing - original draft: T.H., S.H., A.S.N.; Writing - review & editing: T.H., S.H., Y.I., A.S.N.; Visualization: T.H., S.H., A.S.N.; Supervision: A.S.N.; Project administration: A.S.N.; Funding acquisition: A.S.N.

Funding

This research was supported by Japan Society for the Promotion of Science KAKENHI to A.S.N (25440150, 17K19369, 20K06713 and JP22H04827), by Grants-in-Aid from Hirosaki University to A.S.N. (Grant for Exploratory Research by Young Scientists during 2012-2015 and 2017, Institutional Research Grant for Young Investigators 2017-2019, and Interdisciplinary Collaborative Research Grant for Young Scientists in 2018 and 2019), and also in part by the Yamada Science Foundation, the Sumitomo Foundation, and the Sekisui Integrated Research Foundation to A.S.N.

References

Akahoshi, T., Hotta, K. and Oka, K. (2017). Characterization of calcium transients during early embryogenesis in ascidians *Ciona robusta* (*Ciona intestinalis* type A) and *Ciona savignyi*. *Dev. Biol.* **431**, 205-214. doi:10.1016/j.ydbio.2017.09.019

Akahoshi, T., Utsumi, M. K., Oonuma, K., Murakami, M., Horie, T., Kusakabe, T. G., Oka, K. and Hotta, K. (2021). A single motor neuron determines the rhythm of early motor behavior in *Ciona*. *Sci. Adv.* **7**, eabl6053. doi:10.1126/sciadv.abl6053

Anderson, P. A. V. (1979). Ionic basis of action potentials and bursting activity in the hydromedusan jellyfish *Polyorchis penicillatus*. *J. Exp. Biol.* **78**, 299-302. doi:10.1242/jeb.78.1.299

Angstadt, J. D. and Calabrese, R. L. (1989). A hyperpolarization-activated inward current in heart interneurons of the medicinal leech. *J. Neurosci.* **9**, 2846-2857. doi:10.1523/JNEUROSCI.09-08-02846.1989

Athira, A., Dondorp, D., Rudolf, J., Peytral, O. and Chatzigeorgiou, M. (2021). Comprehensive analysis of behavioral dynamics in the protochordate *Ciona intestinalis*. *bioRxiv* 2021.10.29.466420. doi:10.1101/2021.10.29.466420

Bässler, U. (1986). On the definition of central pattern generator and its sensory control. *Biol. Cybern.* **54**, 65-69. doi:10.1007/BF00337116

Bone, Q. (1992). On the locomotion of ascidian tadpole larvae. *J. Mar. Biol. Assoc. UK* **72**, 161-186. doi:10.1017/S0025315400048864

Bostwick, M., Smith, E. L., Borba, C., Newman-Smith, E., Guleria, I., Kourakis, M. J. and Smith, W. C. (2020). Antagonistic inhibitory circuits integrate visual and gravitactic behaviors. *Curr. Biol.* **30**, 600-609.e2. doi:10.1016/j.cub.2019.12.017

Brown, E. R., Nishino, A., Bone, Q., Meinertzhagen, I. A. and Okamura, Y. (2005). GABAergic synaptic transmission modulates swimming in the ascidian larva. *Eur. J. Neurosci.* **22**, 2541-2548. doi:10.1111/j.1460-9568.2005.04420.x

Brunetti, R., Gissi, C., Pennati, R., Caicci, F., Gasparini, F. and Manni, L. (2015). Morphological evidence that the molecularly determined *Ciona intestinalis* type A and type B are different species: *Ciona robusta* and *Ciona intestinalis*. *J. Zool. Syst. Evol. Res.* **53**, 186-193. doi:10.1111/jzs.12101

Buchanan, J. T. and Grillner, S. (1987). Newly identified 'glutamate interneurons' and their role in locomotion in the lamprey spinal cord. *Science* **236**, 312-314. doi:10.1126/science.3563512

Cangiano, L. and Grillner, S. (2003). Fast and slow locomotor burst generation in the hemispinal cord of the lamprey. *J. Neurophysiol.* **89**, 2931-2942. doi:10.1152/jn.01100.2002
Cangiano, L. and Grillner, S. (2005). Mechanisms of rhythm generation in a spinal locomotor network deprived of crossed connections: the lamprey hemicord. *J. Neurosci.* **25**, 923-935. doi:10.1523/JNEUROSCI.2301-04.2005
Cohen, A. H. and Wallén, P. (1980). The neuronal correlate of locomotion in fish. *Exp. Brain Res.* **41**, 11-18. doi:10.1007/BF00236674
Coric, T., Passamaneck, Y. J., Zhang, P., Di Gregorio, A. and Canessa, C. M. (2008). Simple chordates exhibit a proton-independent function of acid-sensing ion channels. *FASEB J.* **22**, 1914-1923. doi:10.1096/fj.07-100313
Crisp, D. J. and Ghobashy, A. F. A. A. (1971). Responses of the larvae of Diplosoma listerianum to light and gravity. In *Fourth European Marine Biology Symposium* (ed. D. J. Crisp), pp. 443-465. U. S. A: Cambridge University Press.
Dale, N. and Roberts, A. (1984). Excitatory amino acid receptors in *Xenopus* embryo spinal cord and their role in the activation of swimming. *J. Physiol.* **348**, 527-543. doi:10.1113/jphysiol.1984.sp015123
Delcomyn, F. (1980). Neural basis of rhythmic behavior in animals. *Science* **210**, 492-498. doi:10.1126/science.7423199
Delcomyn, F. (1998). *Foundations of Neurobiology*. New York, USA: W. H. Freeman & Co.
Durrett, R. (2012). *Essentials of Stochastic Processes*. New York, USA: Springer.
Fetcho, J. R. and McLean, D. L. (2010). Some principles of organization of spinal neurons underlying locomotion in zebrafish and their implications. *Ann. NY. Acad. Sci.* **1198**, 94-104. doi:10.1111/j.1749-6632.2010.05539.x
Gibboney, S., Orvis, J., Kim, K., Johnson, C. J., Martinez-Feduchi, P., Lowe, E. K., Sharma, S. and Stolfi, A. (2020). Effector gene expression underlying neuron subtype-specific traits in the Motor Ganglion of *Ciona*. *Dev. Biol.* **458**, 52-63. doi:10.1016/j.ydbio.2019.10.012
Ghali, M. G. Z. (2019). Respiratory rhythm generation and pattern formation: oscillators and network mechanisms. *J. Integr. Neurosci.* **18**, 481-517. doi:10.31083/j.jin.2019.04.188
Grillner, S. (1975). Locomotion in vertebrates: central mechanisms and reflex interaction. *Physiol. Rev.* **55**, 247-304. doi:10.1152/physrev.1975.55.2.247
Grillner, S. and El Manira, A. (2020). Current principles of motor control with special reference to vertebrate locomotion. *Physiol. Rev.* **100**, 271-320. doi:10.1152/physrev.00015.2019
Grillner, S. and Wallén, P. (1984). How does the lamprey central nervous system make the lamprey swim? *J. Exp. Biol.* **112**, 337-357. doi:10.1242/jeb.112.1.337
Grillner, S., Wallén, P., Brodin, L. and Lansner, A. (1991). Neuronal network generating locomotor behavior in lamprey: circuitry, transmitters, membrane properties, and simulation. *Annu. Rev. Neurosci.* **14**, 169-199. doi:10.1146/annurev.ne.14.030191.001125
Harris-Warrick, R. M. and Johnson, B. R. (2010). Checks and balances in neuromodulation. *Front. Behav. Neurosci.* **4**, 47. doi:10.3389/fnbeh.2010.00047
Horie, T., Kusakabe, T. and Tsuda, M. (2008a). Glutamatergic networks in the *Ciona intestinalis* larva. *J. Comp. Neurol.* **508**, 249-263. doi:10.1002/cne.21678
Horie, T., Sakurai, D., Ohtsuki, H., Terakita, A., Shichida, Y., Usukura, J., Kusakabe, T. and Tsuda, M. (2008b). Pigmented and nonpigmented ocelli in the brain vesicle of the ascidian larva. *J. Comp. Neurol.* **509**, 88-102. doi:10.1002/cne.21733
Horie, T., Nakagawa, M., Sasakura, Y., Kusakabe, T. G. and Tsuda, M. (2010). Simple motor system of the ascidian larva: neuronal complex comprising putative cholinergic and GABAergic/glycinergic neurons. *Zool. Sci.* **27**, 181-190. doi:10.2108/zsj.27.181
Hudson, C. (2016). The central nervous system of ascidian larvae. *Wiley Interdiscip. Rev. Dev. Biol.* **5**, 538-561. doi:10.1002/wdev.239
Imai, J. H. and Meinertzhagen, I. A. (2007). Neurons of the ascidian larval nervous system in *Ciona intestinalis*: I. Central nervous system. *J. Comp. Neurol.* **501**, 316-334. doi:10.1002/cne.21246
Jokura, K., Nishino, J. M., Ogasawara, M. and Nishino, A. (2020). An α7-related nicotinic acetylcholine receptor mediates the ciliary arrest response in pharyngeal gill slits of *Ciona*. *J. Exp. Biol.* **223**, jeb209320. doi:10.1242/jeb.209320
Kajiwara, S. and Yoshida, M. (1985). Changes in behavior and ocellar structure during the larval life of solitary ascidians. *Biol. Bull.* **169**, 565-577. doi:10.2307/1541299
Katz, M. J. (1983). Comparative anatomy of the tunicate tadpole, *Ciona intestinalis*. *Biol. Bull.* **164**, 1-27. doi:10.2307/1541186
Kawai, T., Hashimoto, M., Eguchi, N., Nishino, J. M., Jinno, Y., Mori-Kreiner, R., Aspåker, M., Chiba, D., Ohtsuka, Y., Kawanabe, A. et al. (2021). Heterologous functional expression of ascidian Nav1 channels and close relationship with the evolutionary ancestor of vertebrate Nav channels. *J. Biol. Chem.* **296**, 100783. doi:10.1016/j.jbc.2021.100783
Kiehn, O., Kjaerulff, O., Tresch, M. C. Harris-Warrick, R. M. (2000). Contributions of intrinsic motor neuron properties to the production of rhythmic motor output in the mammalian spinal cord. *Brain Res. Bull.* **53**, 649-659. doi:10.1016/s0361-9230(00)00398-1
Kim, K., Gibboney, S., Razy-Krajka, F., Lowe, E. K., Wang, W. and Stolfi, A. (2020). Regulation of neurogenesis by FGF signaling and neurogenin in the invertebrate chordate *Ciona*. *Front. Cell Dev. Biol.* **8**, 477. doi:10.3389/fcell.2020.00477
Koshiya, N. and Smith, J. C. (1999). Neuronal pacemaker for breathing visualized in vitro. *Nature* **400**, 360-363. doi:10.1038/22540
Kourakis, M. J., Borba, C., Zhang, A., Newman-Smith, E., Salas, P., Manjunath, B. and Smith, W. C. (2019). Parallel visual circuitry in a basal chordate. *Elife* **8**, e44753. doi:10.7554/eLife.44753
Kowalevsky, A. O. (1866). Entwicklungsgeschichte der einfachen Ascidien. *Mem. Acad. Sci. St. Petersbg.* **10**, 1-19.
Liao, J. C. and Fetcho, J. R. (2008). Shared versus specialized glycinergic spinal interneurons in axial motor circuits of larval zebrafish. *J. Neurosci.* **28**, 12982-12992. doi:10.1523/JNEUROSCI.3330-08.2008
Maylie, J. and Morad, M. (1984). Ionic currents responsible for the generation of pace-maker current in the rabbit sino-atrial node. *J. Physiol.* **355**, 215-235. doi:10.1113/jphysiol.1984.sp015415
McHenry, M. J. and Patek, S. N. (2004). The evolution of larval morphology and swimming performance in ascidians. *Evolution* **58**, 1209-1224. doi:10.1111/j.0014-3820.2004.tb01701.x
Meinertzhagen, , I. A., Lemaire, P. and Okamura, Y. (2004). The neurobiology of the ascidian tadpole larva: recent developments in an ancient chordate. *Annu. Rev. Neurosci.* **27**, 453-485. doi:10.1146/annurev.neuro.27.070203.144255
Nakagawa, M., Miyamoto, T., Ohkuma, M. and Tsuda, M. (1999). Action spectrum for the photophobic response of *Ciona intestinalis* (Ascidieacea. Urochordata) larvae implicates retinal protein. *Photochem. Photobiol.* **70**, 359-362. doi:10.1111/j.1751-1097.1999.tb08149.x
Navarrete, I. A. and Levine, M. (2016). Nodal and FGF coordinate ascidian neural tube morphogenesis. *Development* **143**, 4665-4675. doi:10.1242/dev.144733
Nishino, A. (2018). Morphology and physiology of the ascidian nervous systems and the effectors. In *Transgenic Ascidians* (ed. Y. Sasakura), pp. 179-196. Singapore: Springer.
Nishino, A., Okamura, Y., Piscopo, S. and Brown, E. R. (2010). A glycine receptor is involved in the organization of swimming movements in an invertebrate chordate. *BMC Neurosci.* **11**, 6. doi:10.1186/1471-2202-11-6
Nishino, A., Baba, S. A. and Okamura, Y. (2011). A mechanism for graded motor control encoded in the channel properties of the muscle ACh receptor. *Proc. Natl. Acad. Sci. USA* **108**, 2599-2604. doi:10.1073/pnas.1013547108
Nishitsuji, K., Horie, T., Ichinose, A., Sasakura, Y., Yasuo, H. and Kusakabe, T. G. (2012). Cell lineage and cis-regulation for a unique GABAergic/glycinergic neuron type in the larval nerve cord of the ascidian *Ciona intestinalis*. *Dev. Growth Differ.* **54**, 177-186. doi:10.1111/j.1440-169x.2011.01319.x
Ohmori, H. and Sasaki, S. (1977). Development of neuromuscular transmission in a larval tunicate. *J. Physiol.* **269**, 221-254. doi:10.1113/jphysiol.1977.sp011900
Okada, T., Katsuyama, Y., Ono, F. and Okamura, Y. (2002). The development of three identified motor neurons in the larva of an ascidian, *Halocynthia roretzi*. *Dev. Biol.* **244**, 278-292. doi:10.1006/dbio.2002.0585
Pan, B. (2011). Recent progress in digital image correlation. *Exp. Mech.* **51**, 1223-1235. doi:10.1007/s11340-010-9418-3
Passamaneck, Y. J., Hadjantonakis, A. K. and Di Gregorio, A. (2007). Dynamic and polarized muscle cell behaviors accompany tail morphogenesis in the ascidian *Ciona intestinalis*. *PLoS One* **2**, e714. doi:10.1371/journal.pone.0000714
Picton, L. D., Sillar, K. T. and Zhang, H.-Y. (2018). Control of *Xenopus* tadpole locomotion via selective expression of Ih in excitatory interneurons. *Curr. Biol.* **28**, 3911-3923.e2. doi:10.1016/j.cub.2018.10.048
Poon, M. L. T. (1980). Induction of swimming in lamprey by L-DOPA and amino acids. *J. Comp. Physiol. A* **136**, 337-344. doi:10.1007/BF00657354
Razy-Krajka, F. and Stolfi, A. (2019). Regulation and evolution of muscle development in tunicates. *EvoDevo* **10**, 13. doi:10.1186/s13227-019-0125-6
Roberts, A. (2000). Early functional organization of spinal neurons in developing lower vertebrates. *Brain Res. Bull* **53**, 585-593. doi:10.1016/S0361-9230(00)00392-0
Roberts, A., Li, W.-C. and Soffe, S. R. (2010). How neurons generate behavior in a hatchling amphibian tadpole: an outline. *Front. Behav. Neurosci.* **4**, 16. doi:10.3389/fnbeh.2010.00016
Rudolf, J., Dondorp, D., Canon, L., Tieo, S. and Chatzigeorgiou, M. (2019). Automated behavioural analysis reveals the basic behavioural repertoire of the urochordate *Ciona intestinalis*. *Sci. Rep.* **9**, 2416. doi:10.1038/s41598-019-38791-5
Ryan, K., Lu, Z. and Meinertzhagen, I. A. (2016). The CNS connectome of a tadpole larva of *Ciona intestinalis* (L.) highlights sidedness in the brain of a chordate sibling. *Elife* **5**, e16962. doi:10.7554/eLife.16962
Ryan, K., Lu, Z. and Meinertzhagen, I. A. (2017). Circuit homology between decussating pathways in the *Ciona* larval CNS and the vertebrate startle-response pathway. *Curr. Biol.* **27**, 721-728. doi:10.1016/j.cub.2017.01.026
Ryan, K., Lu, Z. and Meinertzhagen, I. A. (2018). The peripheral nervous system of the ascidian tadpole larva: types of neurons and their synaptic networks. *J. Comp. Neurol.* **526**, 583-608. doi:10.1002/cne.24353
Salas, P., Vinaithirthan, V., Newman-Smith, E., Kourakis, M. J. and Smith, W. C. (2018). Photoreceptor specialization and the visuomotor repertoire of the primitive chordate *Ciona*. *J. Exp. Biol.* **221**, jeb177972. doi:10.1242/jeb.177972

Satoh, N. (2003). The ascidian tadpole larva: comparative molecular development and genomics. *Nat. Rev. Genet.* **4**, 285-295. doi:10.1038/nrg1042

Satoh, N., Rokhsar, D. and Nishikawa, T. (2014). Chordate evolution and the three-phylum system. *Proc. R. Soc. B* **281**, 20141729. doi:10.1098/rspb.2014.1729

Satou, C., Sugioka, T., Uemura, Y., Shimazaki, T., Zmarz, P., Kimura, Y. and Higashijima, S.-I. (2020). Functional diversity of glycinergic commissural inhibitory neurons in larval zebrafish. *Cell Rep.* **30**, 3036-3050.e4. doi:10.1016/j.celrep.2020.02.015

Smith, J. C., Ellenberger, H. H., Ballanyi, K., Richter, D. W. and Feldman, J. L. (1991). Pre-Bötzinger complex: a brainstem region that may generate respiratory rhythm in mammals. *Science* **254**, 726-729. doi:10.1126/science.1683005

Stolfi, A. and Levine, M. (2011). Neuronal subtype specification in the spinal cord of a protovertebrate. *Development* **138**, 995-1004. doi:10.1242/dev.061507

Stolfi, A., Ryan, K., Meinertzhagen, I. A. and Christiaen, L. (2015). Migratory neuronal progenitors arise from the neural plate borders in tunicates. *Nature* **527**, 371-374. doi:10.1038/nature15758

Svane, I. and Young, C. M. (1989). The ecology and behaviour of ascidian larvae. *Oceanogr. Mar. Biol. Annu. Rev.* **27**, 45-90.

Thoby-Brisson, M., Telgkamp, P. and Ramirez, J.-M. (2000). The role of the hyperpolarization-activated current in modulating rhythmic activity in the isolated respiratory network of mice. *J. Neurosci.* **20**, 2994-3005. doi:10.1523/JNEUROSCI.20-08-02994.2000

Tsuda, M., Sakurai, D. and Goda, M. (2003a). Direct evidence for the role of pigment cells in the brain of ascidian larvae by laser ablation. *J. Exp. Biol.* **206**, 1409-1417. doi:10.1242/jeb.00235

Tsuda, M., Kawakami, I. and Shiraishi, S. (2003b). Sensitization and habituation of the swimming behavior in ascidian larvae to light. *Zool. Sci.* **20**, 13-22. doi:10.2108/zsj.20.13

Tytell, E. D., Holmes, P. and Cohen, A. H. (2011). Spikes alone do not behavior make: why neuroscience needs biomechanics. *Curr. Opin. Neurobiol.* **21**, 816-822. doi:10.1016/j.conb.2011.05.017

Wiggin, T. D., Anderson, T. M., Eian, J., Peck, J. H. and Masino, M. A. (2012). Episodic swimming in the larval zebrafish is generated by a spatially distributed spinal network with modular functional organization. *J. Neurophysiol.* **108**, 925-934. doi:10.1152/jn.00233.2012

Wiggin, T. D., Peck, J. H. and Masino, M. A. (2014). Coordination of fictive motor activity in the larval zebrafish is generated by non-segmental mechanisms. *PLoS One* **9**, e109117. doi:10.1371/journal.pone.0109117

Yokoyama, T. D., Hotta, K. and Oka, K. (2014). Comprehensive morphological analysis of individual peripheral neuron dendritic arbors in ascidian larvae using the photoconvertible protein Kaede. *Dev. Dyn.* **243**, 1362-1373. doi:10.1002/DVDY.24169

Zega, G., Thorndyke, M. C. and Brown, E. R. (2006). Development of swimming behaviour in the larva of the ascidian *Ciona intestinalis*. *J. Exp. Biol.* **209**, 3405-3412. doi:10.1242/jeb.02421

Zega, G., Biggiogero, M., Groppelli, S., Candiani, S., Oliveri, D., Parodi, M., Pestarino, M., De Bernardi, F. and Pennati, R. (2008). Developmental expression of glutamic acid decarboxylase and of γ-aminobutyric acid type B receptors in the ascidian *Ciona intestinalis*. *J. Comp. Neurol.* **506**, 489-505. doi:10.1002/cne.21565